

## CHAPTER III

### RESULTS AND DISCUSSION

#### 3.1 High Density Polyethylene

The morphology of a fracture surface can indicate the direction of crack growth and the approximate velocity of the crack. The impacted specimens with a notch depth of 2.5 mm were hit by a single swing of the pendulum. All of the HDPE specimens showed crack growth along the direction of the stress induced by pendulum but all of the cracked specimens were incompletely broken. According to ASTM 256, this type of failure is called partial break.

##### 3.1.1 Fractography of High Density Polyethylene

Four characteristic regions have been identified for the HDPE impact fracture surface in this study. The fracture first started at the notch. There were half circular regions, patchy regions, discontinuous growth bands and a fast fracture region as showed in Figure 3.1. The discontinuous growth bands commonly occur on fatigue fracture surfaces depending on the molecular weight of a particular polymer (Mark et al., 1985).

In other fractures, tensile rupture of all HDPE specimens showed the ductile deformation generally involves a more extended region than other brittle material. The tensile fracture of HDPE showed necking and drawing that drawn out more than 30 cm. The long-chain nature of polymer molecules requires that the most preferred slip plane in polymer crystals contains the

molecular chain. The polyethylene chains can remain unbroken through very large deformations (Lin and Argon 1994).

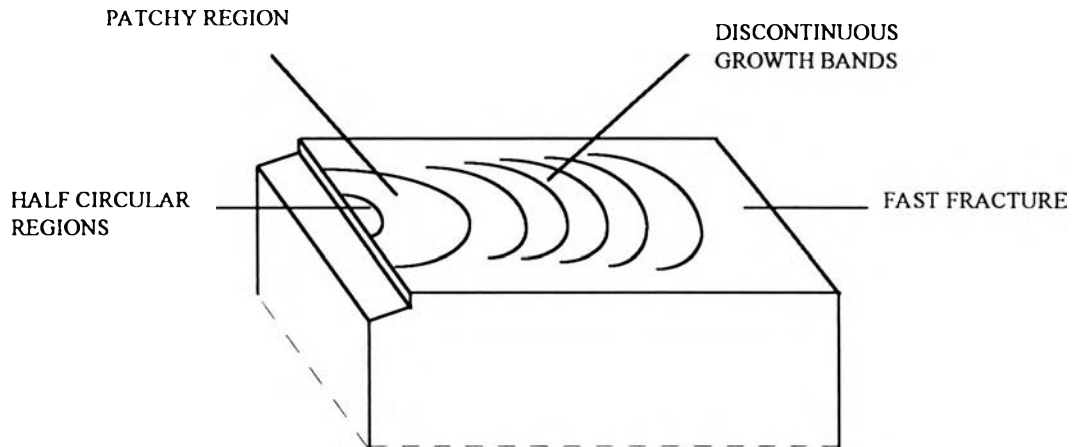


**Figure 3.1** A schematic of impact fracture surface of HDPE semicrystalline polymer.

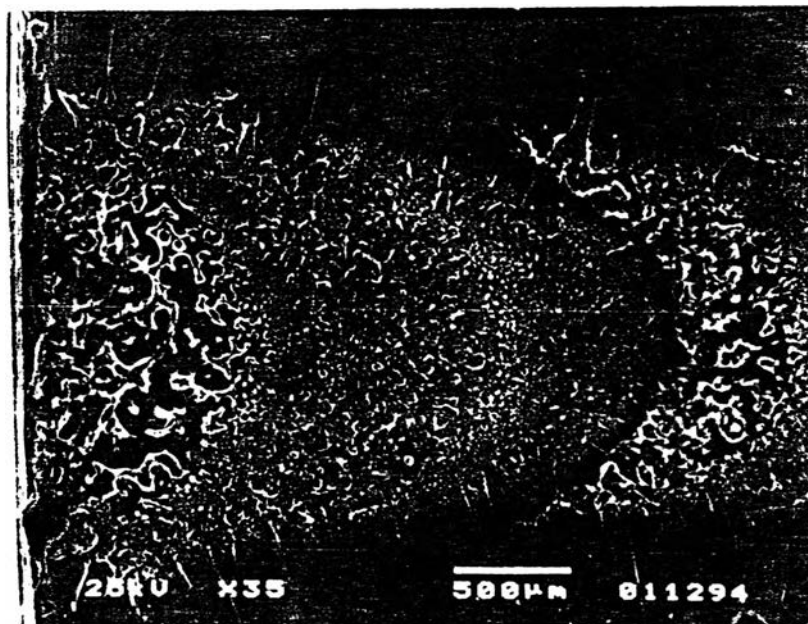


**Figure 3.2** SEM photograph of half circular region and patchy region of impact fracture surface of HDPE.

The origin of the impact fracture is located at the notch where the stress concentration in the specimen takes place. The half circular region appeared beyond the notch as a result of high stress in the first crack. In the half circular region polymer were drawn and some of the drawn polymer contracted after rupture. Next to the half circular region, the fracture exhibited a patchy region with features in the range of 20-170  $\mu\text{m}$ , as seen in Figure 3.2.

In the crack propagation region, discontinuous growth bands were observed with striation bands perpendicular to the direction of crack growth. Furthermore the discontinuous growth bands were spread out from the center to near the edge of the specimen. The maximum stress is at the center that is the point of the crack initiated in each band. Then the stress transfers from center to edge of specimen. The remaining stress at the center can initiate the next step of cracking. Figure 3.1 shows the radius of crack front curve increase along the crack direction.

The fracture surface in each step of crack propagation showed a wavy pattern along the crack growth. Thus the crack propagation of HDPE as observed through SEM can be divided into two zones that are different in crack pattern and crack velocity. In the first zone, surface fracture was caved at the surface exhibiting smooth fracture with a high crack velocity as shown on the left of Figure 3.3 (b). The other zone is shown on the right of Figure 3.3 (b), the polymer was drawn and some contracted after rupture. The fibrillar materials are about 80-100  $\mu\text{m}$ .

After the crack propagation, fast fracture occurred as the third region. The micrograph of impact fracture surface is evident as a smooth area on the final region of the crack growth. This is often observed in the final region of

the fracture surface of other materials such as PMMA and PVC (Wolock and Newman, 1964 and Lee et al., 1987).

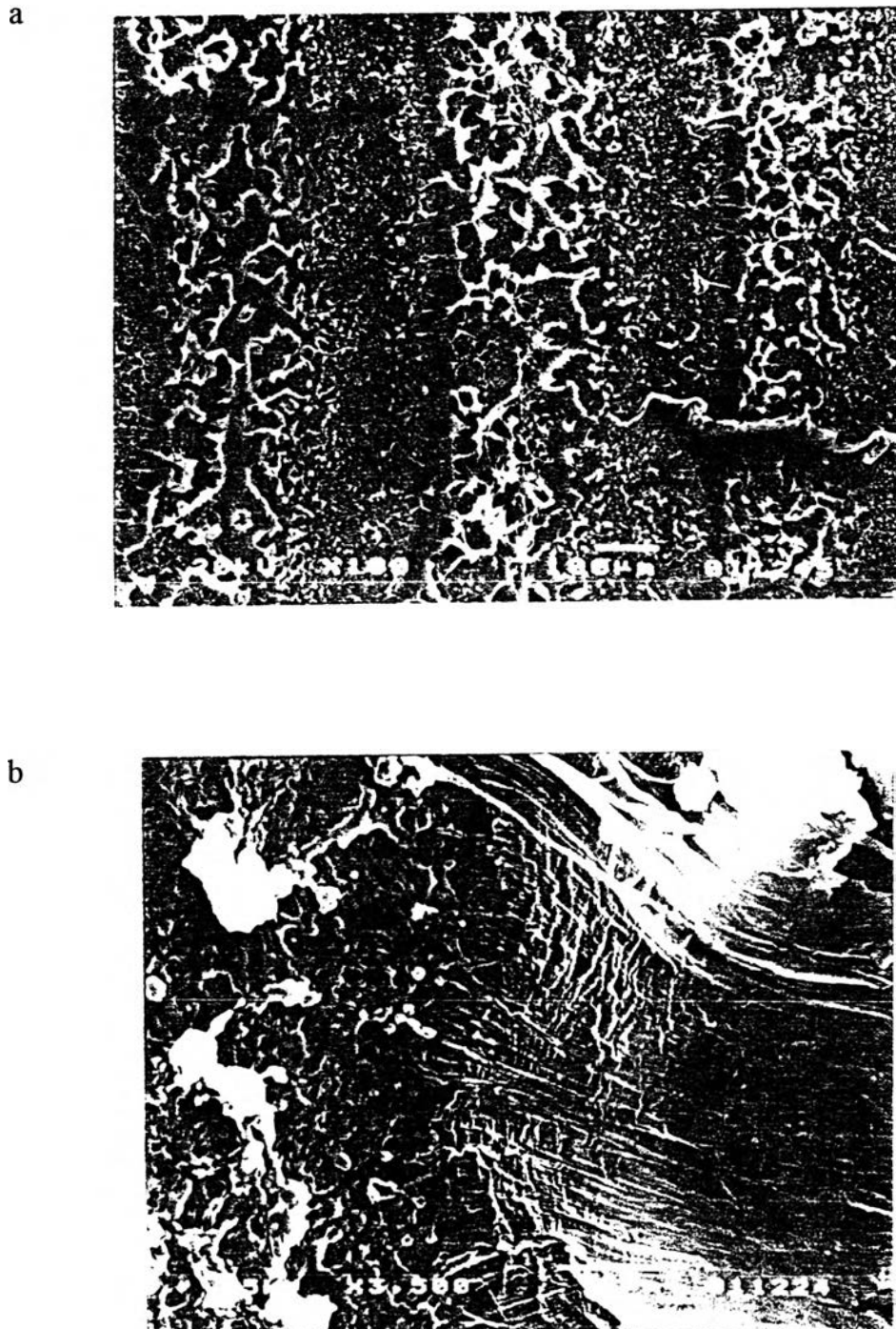


**Figure 3.3** SEM photograph of propagation region of impact fracture surface of HDPE (a) x100 (b) x3500.

### 3.1.2 Effects of Processing History

The impacted fracture surface of virgin and reprocessed HDPE are shown in Figure 3.4(a) and 3.4(b) respectively. The micrograph of both materials shows discontinuous growth bands. But, the width of the striation bands is reduced after reprocessing. In PMMA materials, the ribs increased in number when the molecular weight decreased (Wolock, 1964).

Many studies have reported that chain branching and chain scission can occur during processing due to the high temperatures and shear forces applied to the viscous polymer melt (Grassie and Scott, 1985). According to melt flow index data, following ASTM 2855, the melt flow index of HDPE decreases after reprocessing 10 passes (Arthasart, 1996). This result indicates that the molecular weight of HDPE increased after reprocessing. The melt flow index data suggested that chain branching or chain crosslinking dominated during extrusion through a die. Both reactions of polymer are dependent both on chemical structure and morphology (Scott, 1995). Thus the reduction of the width of the striation bands may come from the chain crosslinking or chain branching but the crystallinity of the material showed no significant change.

The HDPE post consumer bottles were ground to small chips and reprocessed by a twin screw extruder. The micrograph at low magnification in Figure 3.5 still shows the half circular region, discontinuous growth bands and patchy type structure. In addition, fractures in post consumer materials exhibit some impurity inside the texture. Figure 3.6 shows the patchy region of post consumer materials that often initiated from apparent impurity particles. Although there were many defects in the texture of the post-

consumer materials, the mechanical properties, impact strength and tensile strength did not show any significant change.

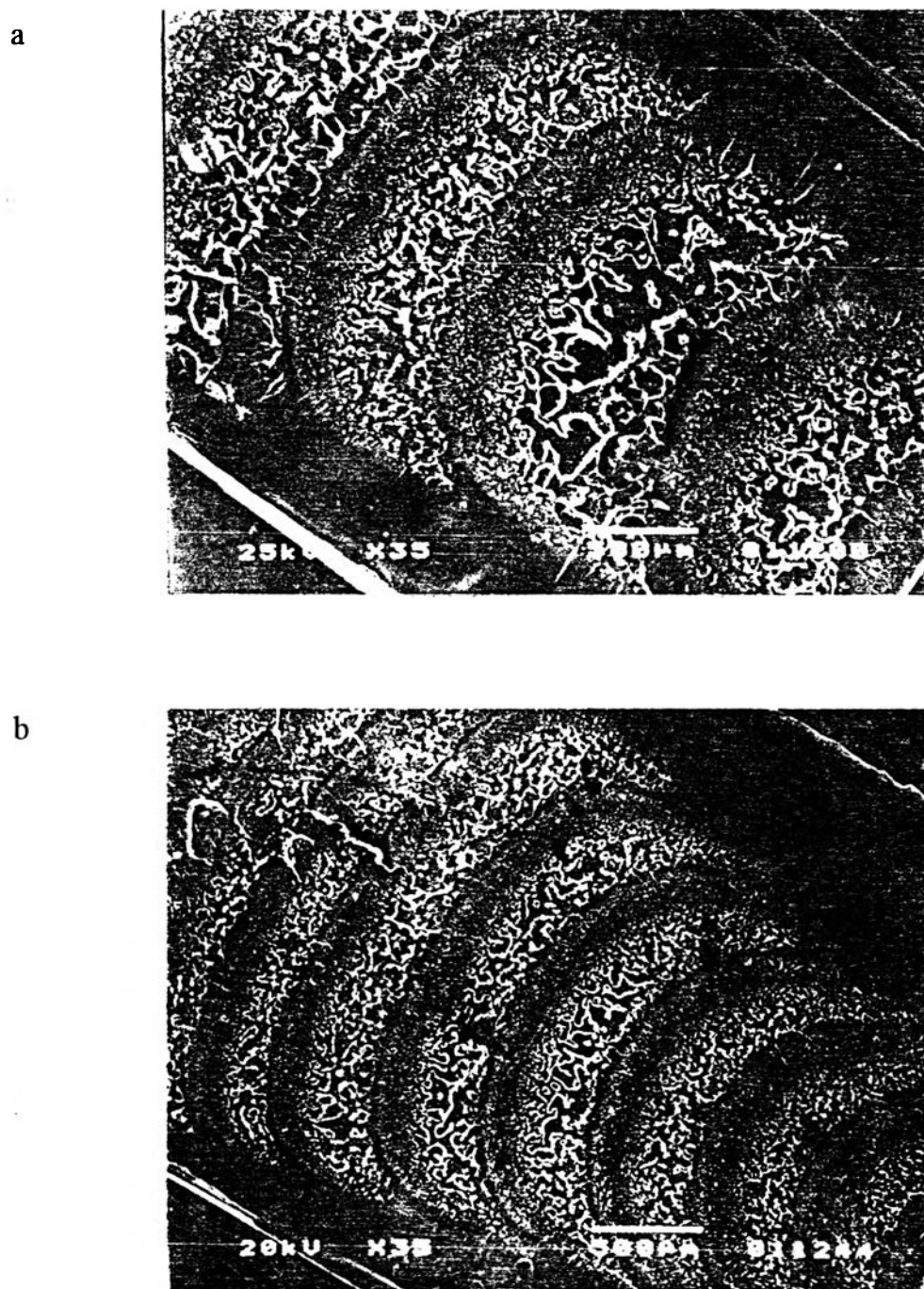


**Figure 3.4** SEM photograph of impact fracture surface of HDPE (a) Virgin (b) Reprocessed material.

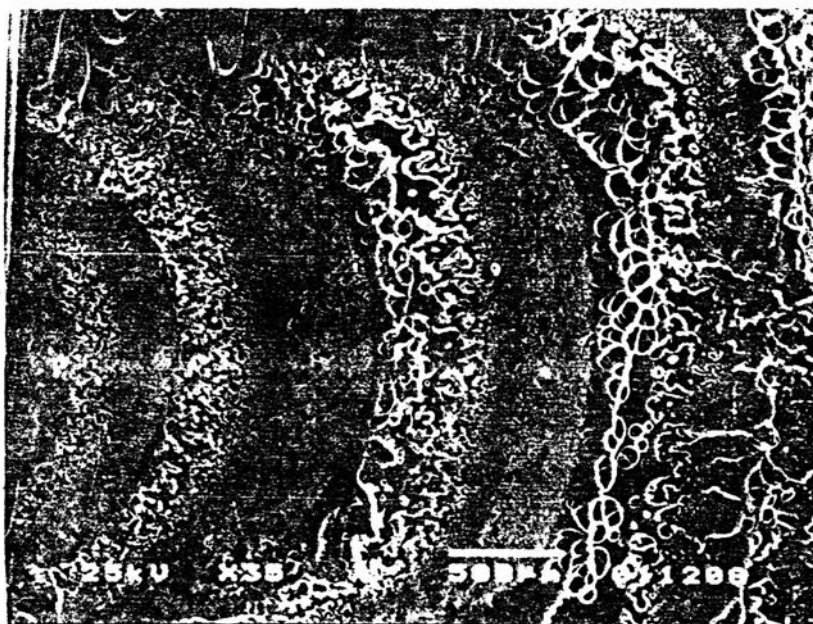
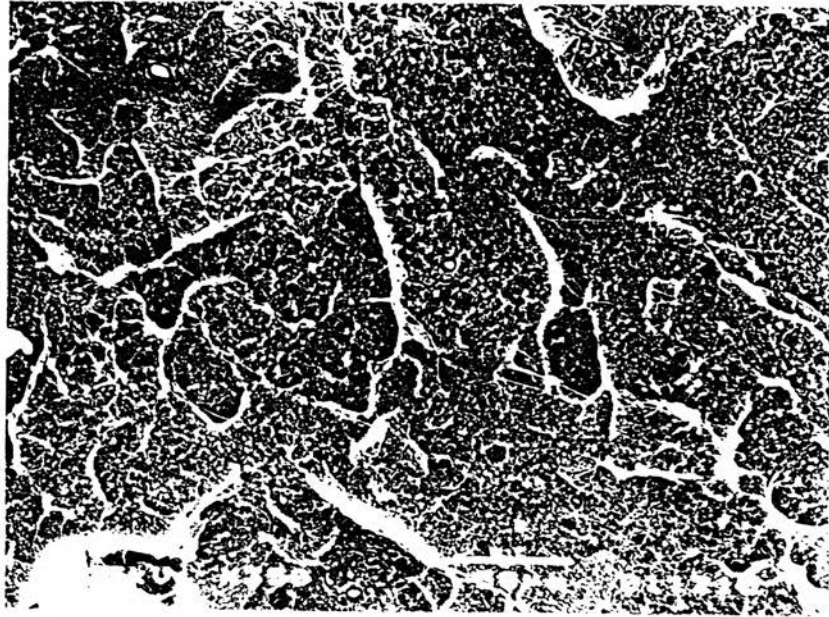


**Figure 3.5** SEM photograph of post-consumer HDPE showing the discontinuous growth bands of impact fracture surface.

a



b

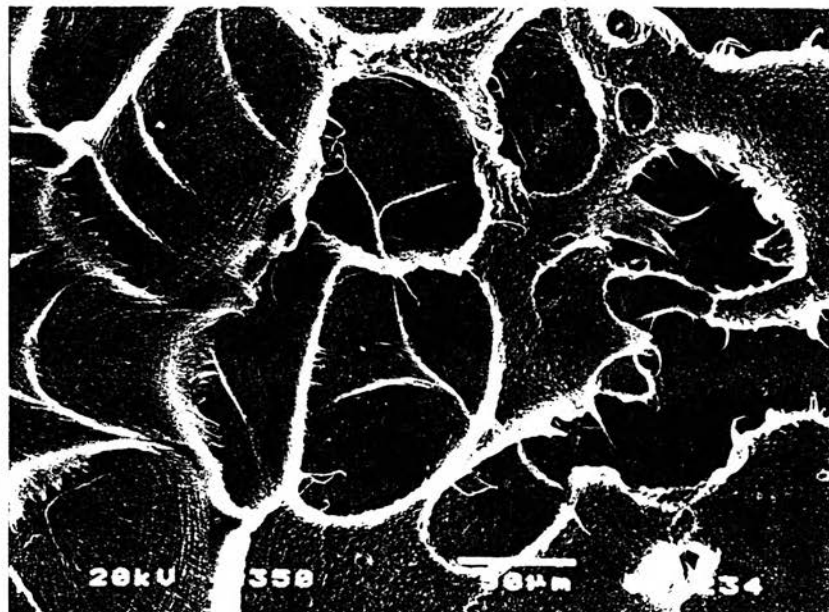


**Figure 3.6** SEM photograph showing impurity of the impact fracture surface in (a) patchy region (b) discontinuous growth bands.

## 3.2 HDPE and PET Blends

Morphological features of the fracture of binary blends and ternary blends were examined using SEM. Typical impact fracture surfaces of the binary blends at low composition of PET are shown in Figures 3.7 for the blends ratio 95/5. The PET particles are spherical or ellipsoidal dispersed in HDPE matrix with very little adhesion. Some holes were seen where the PET spheres have been removed from the other half of the fracture. Figure 3.8(a) shows that the diameters of individual PET particles are in the range of 0.5-2.5  $\mu\text{m}$ .

When the PET was added into the HDPE the fractography of HDPE materials changed dramatically. The half circular region, discontinuous growth bands and the fast fracture surface disappeared. The fractography of polymer blends were not uniform. The patchy regions of the blends were 30-90  $\mu\text{m}$ . There were some PET particles aligned in the same direction within individual patchy regions as shown in Figure 3.7(a).

### 3.2.1 Effects of Processing History

After reprocessing 5 passes of binary blends 5% PET also exhibited a patchy type fracture surface as showed in Figure 3.7(b). At first glance, it appeared that the fractography did not distinguish the fracture surface of the initial blends and the reprocessed 5 passes of blends. There was no change in the size of the patchy areas but they often appeared to initiate from a large PET particles. Some of the PET particles were segregated and some were aggregated. Thus, the distribution of particle size was wider, in range 0.24-4  $\mu\text{m}$  and the alignment of PET particles observed in initial blends disappeared

as shown in Figure 3.8(b). As reported in the previous studies, processing reduced the apparent amount of dispersed phase (Utracki, 1991).

a



b

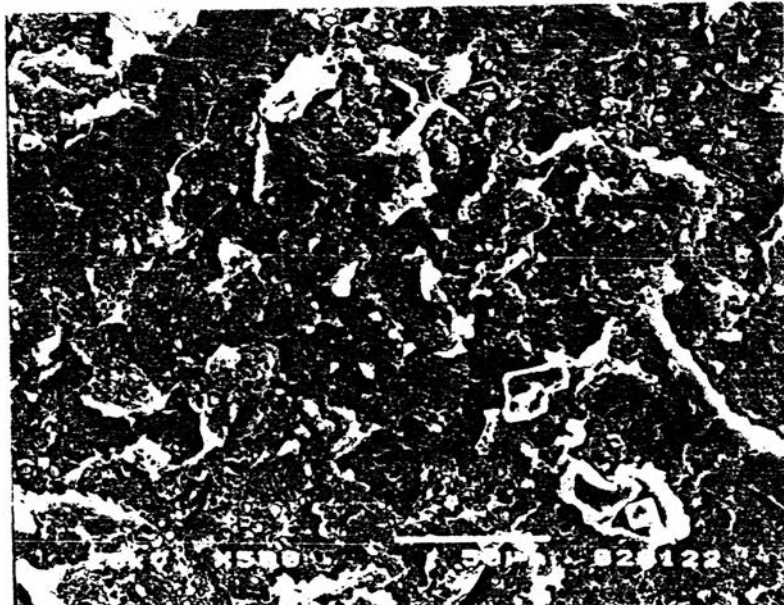
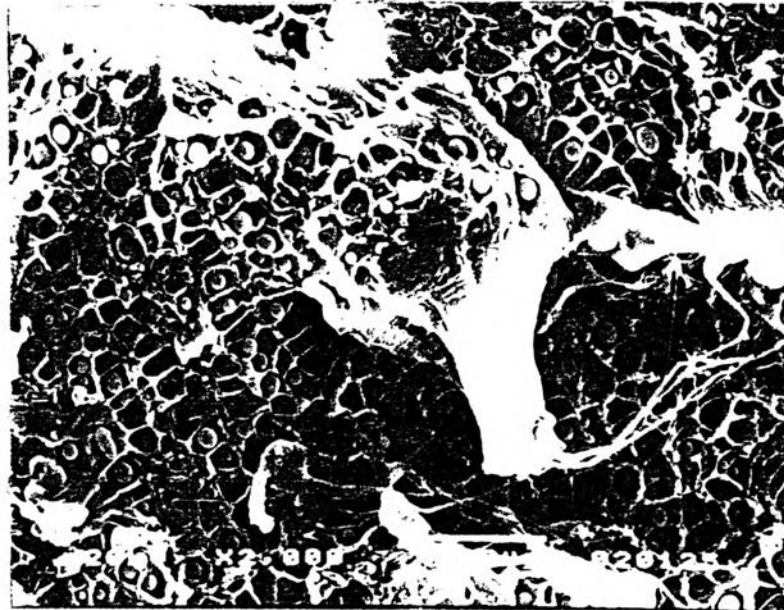


**Figure 3.7** SEM photograph of impact fracture surface of HDPE/PET blends at ratio 95/5 (x500) (a) initial processed (b) reprocessed 5 passes.

a



b

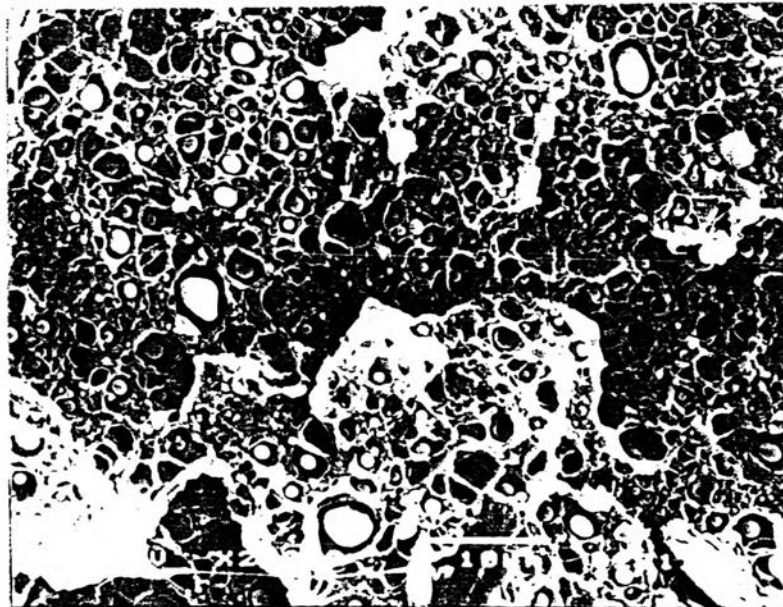


**Figure 3.8** SEM photograph of impact fracture surface of HDPE/PET blends at ratio 95/5 (x2,000) (a) initial processed (b) reprocessed 5 passes.

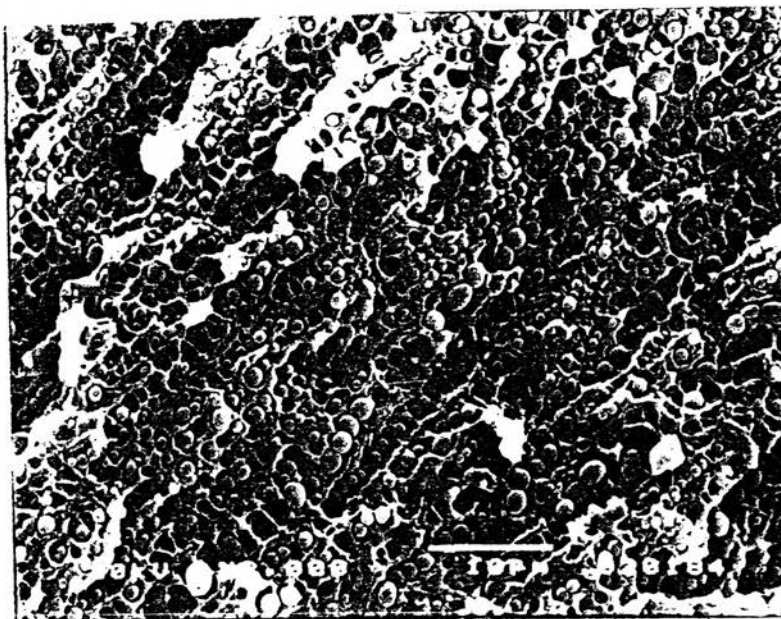
These morphological features can be correlated with impact resistance. The impact resistance of blends of 5% PET decreases from 6.44 kJ/m<sup>2</sup> to 4.30 kJ/m<sup>2</sup> after reprocessing 5 passes. That is the result of the aggregated particles that initiated the patchy region. The large particles were the source of material weaknesses, which cracks can easily nucleate. Thus, the impact resistance of reprocessed specimens were lower than that of the initial blends.

### **3.2.2 Ternary Blends : HDPE/PET/MA**

With the addition of maleic anhydride olefin grafted copolymer as a compatibilizing agent, ternary blends can be obtained which display better mechanical properties (Chen and Lai, 1994, Jabarin et al.,1990). Some differences between the morphology of binary blends and ternary blends may be observed in Figures 3.9(a) and (b). By adding maleic anhydride, it was found that the shape of PET particles were spherical suggesting an improved adhesion between the two components (Chen and Lai, 1994). Figure 3.10(a) shows fracture on the PET particles since they adhere to the other half of fracture. It should be note that a higher ratio of both ternary blends and binary blends, the fracture surface did not show the uniform morphology.

The microstructure of tensile fracture surfaces of ternary blends at ratio 75/20/5 exited some fibril adhesion between the two phases. Figure 3.10(b) shows that PET particles adhere with the drawn HDPE. These micrographs indicated the ternary blends of HDPE, PET and maleic anhydride copolymer were partially compatible.

a



b

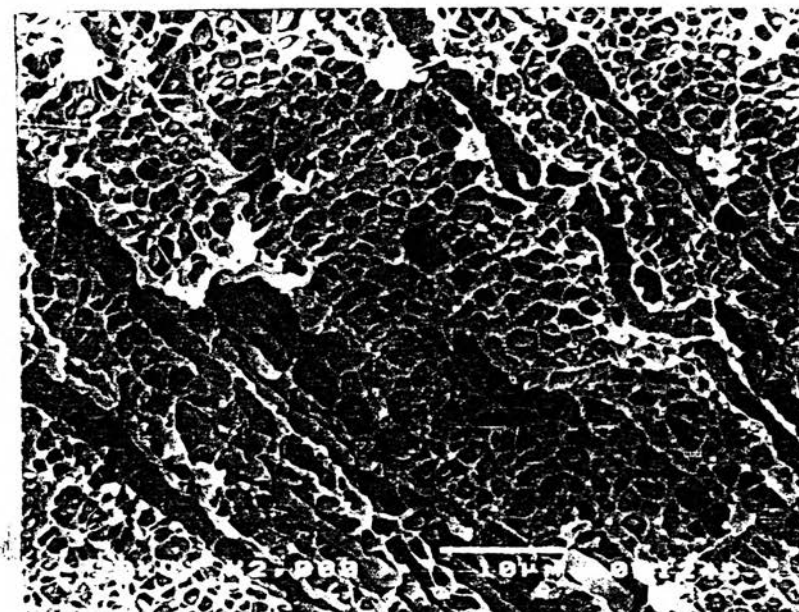
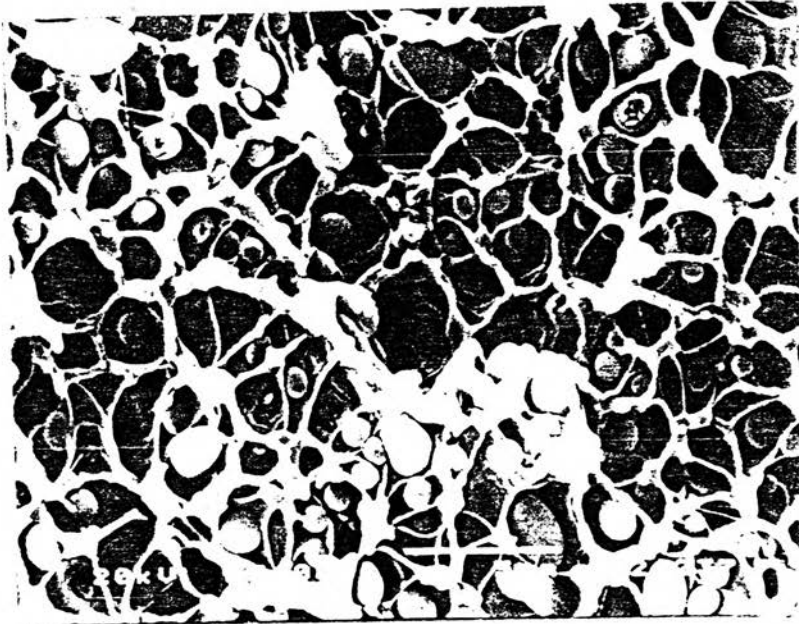


**Figure 3.9** SEM photograph of (a) binary blends at ratio 90/10 and (b) ternary blends at ratio 85/10/5.

a



b



**Figure 3.10** SEM photograph of ternary blends (x5,000) (a) impact fracture surface at ratio 75/20/5 of (b) tensile fracture surface at ratio 75/20/5.

### 3.3 Nylon 6,6

Nylon 6,6 is an important engineering resin because of its toughness over a wide range of temperature, as well as its high impact and abrasion resistance (Mark et al., 1985). At temperature below  $T_g$  the energy absorption is mainly in the notch region. This energy absorption is the crack initiation step (Collyer, 1994).

In this study the toughness was investigated by notched Izod methods at room temperature. All of the samples were dried before molding. At 80 percent of the whole fracture area in impacted samples became stress whitened, while the fracture surface over the rest of sample is smooth. A new plane of crack was generated as shown in the schematic in Figure 3.11. According to ASTM D256 method, the impacted samples were defined as completely broken, since the specimens were broken into two or more pieces.

#### 3.3.1 Fractography of Nylon 6,6

The impact fracture surface of broken specimens of Nylon 6,6 as observed through SEM, can be divided into three regions, the mirror region, the hackle region, and the secondary crack as shown in Figure 3.11.

The mirror region was close to the notch where the fracture started, zone A in Figure 3.13. Figure 3.14 shows the fracture surface area near the notch of a nylon specimen after being impacted by Izod tests. The mirror region appeared in the shape of an ellipse. Collyer (1994) and Wolock (1964) reported that the mirror region size depends on the conditions of fracture, such as temperature and environment and molecular weight of the sample.

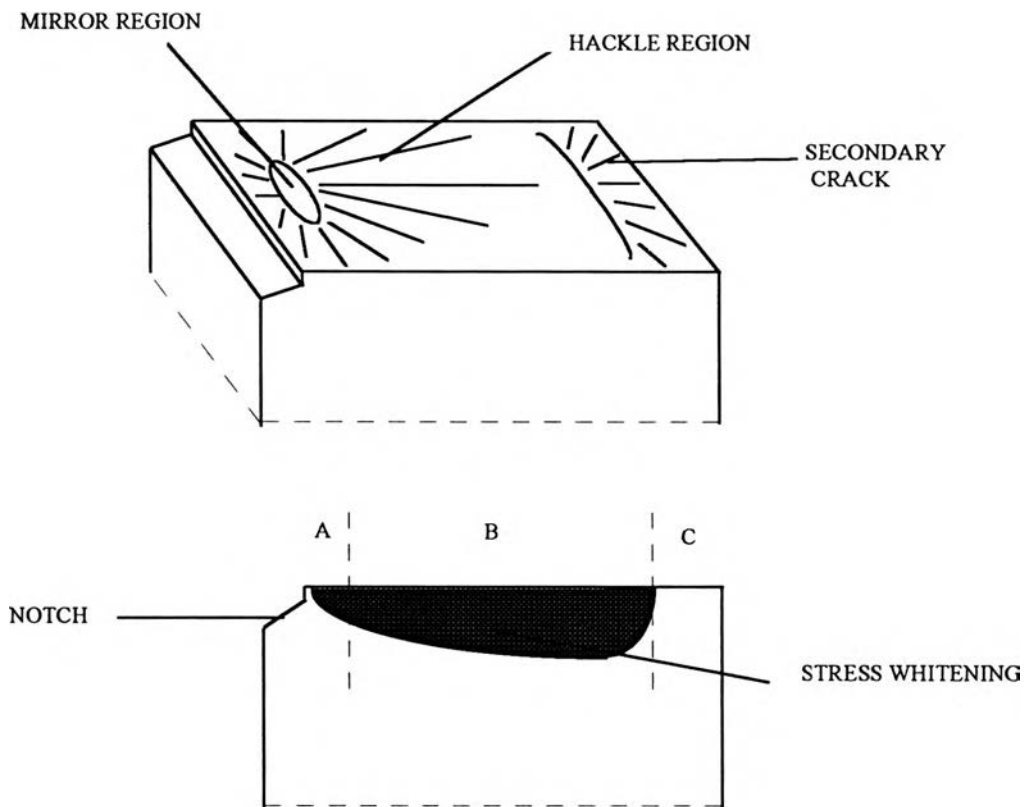


**Figure 3.11** A schematic of impact fracture surface of Nylon 6,6: (a) impact fracture surface;(b) impact break.

The crack propagation beyond the mirror region into zone B was easily recognized by the outwardly divergent lines pointing along the crack propagation direction. Unlike the mirror region, the hackle region exhibited a rough surface as exhibited in Figure 3.12, and Figure 3.13 at higher magnification.



**Figure 3.12** SEM photograph of impact fracture surface showed mirror region and hackle lines of Nylon 6,6.

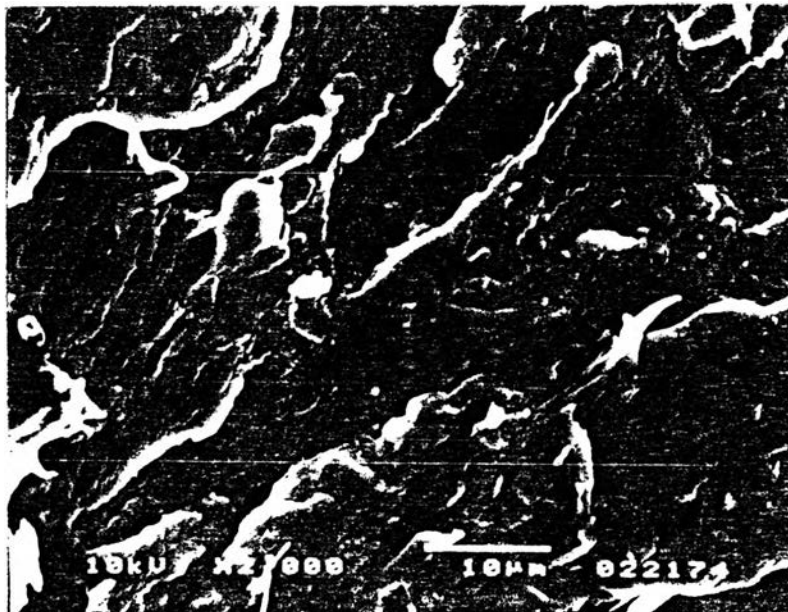


**Figure 3.13** SEM photograph of hackle lines at higher magnification.

Cracking is a stress-relief mechanism for a solid. Elastic strain energy is released during crack extension, providing the crack driving force. As the driving force increases, the crack is driven to higher velocities. The velocity of propagation approaches the limiting velocity in the material. The rapidly moving crack tends to branch into two or more fracture surface areas (So, 1988), as shown in Figure 3.13. Here, hackle lines form as a result of crack front branching. In zone B, it should be noted that the hackle regions are smoother along the crack direction.

In zone C, the micrograph of impact fracture surface shows secondary cracks. The secondary cracks exist in perpendicular to plane of the crack. Secondary crack initiation is preceded by craze formation. Therefore parabolic markings on the surface exist because the weakened craze on the different planes merged with the main crack (So, 1988). Figure 3.14 shows that the crack was initiated by the craze containing an interpenetrating network of voids among highly drawn polymer fibrils bridging the craze face.

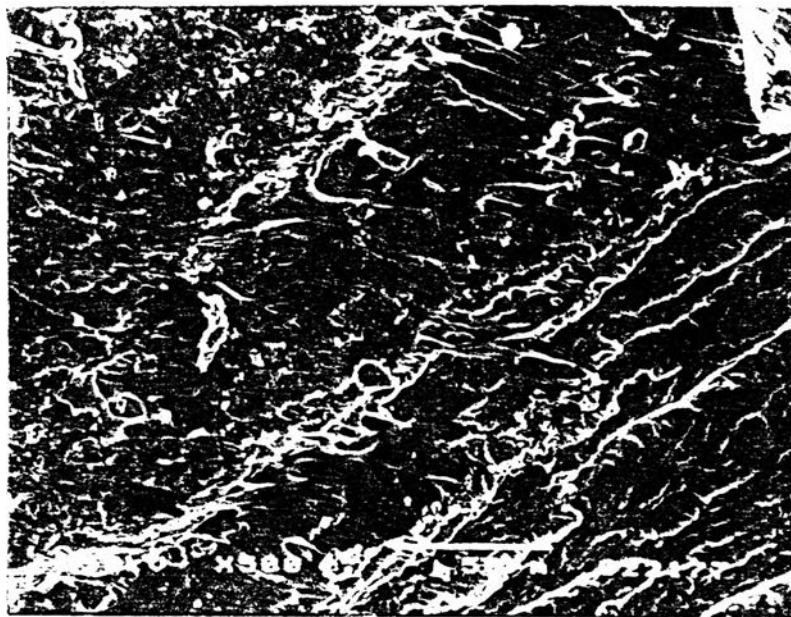
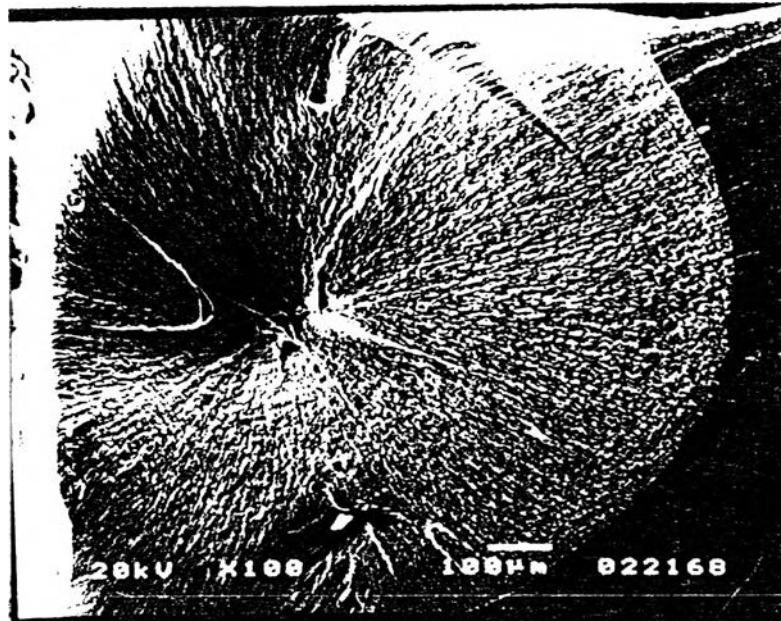


**Figure 3.14** SEM photograph of impact fracture surface showing secondary crack of Nylon 6,6.

### 3.3.2 Tensile Fracture Surface of Nylon 6,6

A tensile test specimen containing no stress concentration is stretched at constant rate until fracture. The stress in the specimen is essentially uniform uniaxial tension (So, 1988). The deformation of tensile fracture surface was initiated by a defect in the specimen as shown in Figure 3.15(a). Moreover the parabolic markings were exited on the fracture surface. Figure 3.15(b) indicates some nucleation in the tensile fracture surface during the specimens were slow stretched at a constant rate, 50.8 mm/min. This nucleation was initiated by the defects in the specimen. The defects in polymers can be impurities, material decomposition, or polymer segregation that nucleate a small particles.

a



b

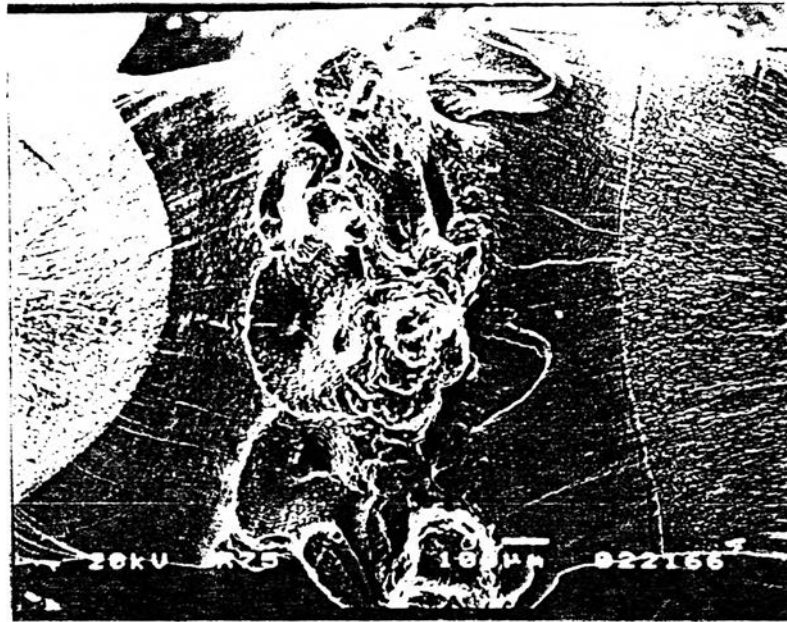
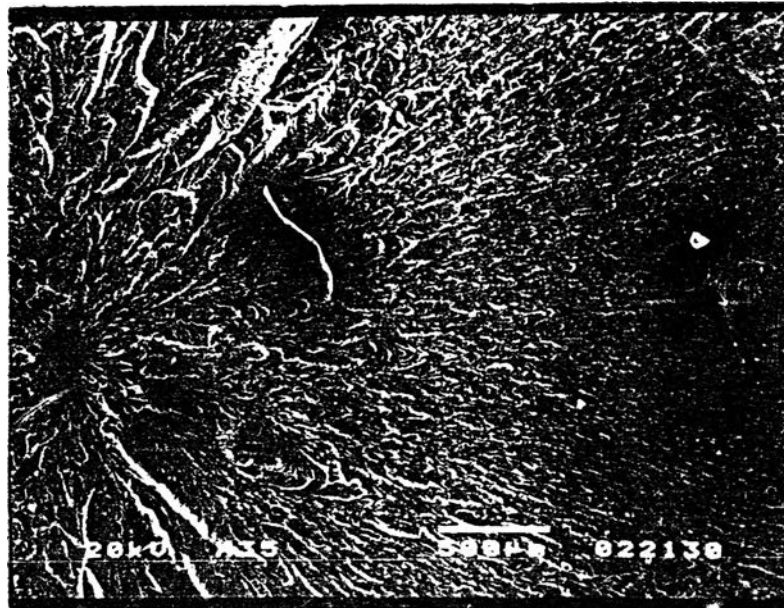


**Figure 3.15** SEM photograph of tensile fracture surface of Nylon 6,6  
 (a) cracks generate by defect (b) nucleation during specimen was stretched.

### 3.3.3 Effects of Processing History

The photomicrographs show reduction in the size of the mirror region after reprocessing 10 passes. This phenomenon can be due to the change of molecular weight as others have reported (Collyer, 1994). Thermo-oxidation can occur at high temperatures. The reaction undergoes by NH transfer generating many kinds of degradation products (Scott, 1995). The thermo-oxidation is also the cause of a reduction in molecular weight and the variability in molecular weight distribution. Correlated to the DSC and impact test results, crystallinity is slightly increased after reprocessing while impact resistance is decreased.

a



b

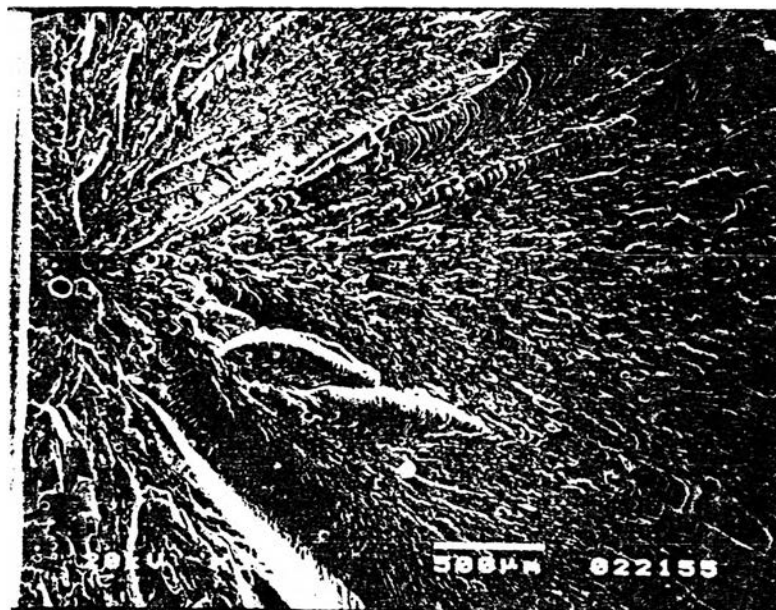


Figure 3.16 SEM photograph comparing impact fracture surface between virgin and reprocessed Nylon 6,6.

The micrograph showed the increment in quantity and length of outwardly divergent lines or hackle lines after reprocessing 10 passes as seen in Figure 3.16. Since the processing operation causes a significant decrease in the spherulite diameter and the crazes appear to initiate or grow preferentially at either the center or edge of the spherulite (Khanna et al.,1998, Wyzgoski and Novak, 1992).

### **3.4 Polyetherimide**

Polyetherimide (PEI) is an amorphous high performance thermoplastic. The chemical structure of PEI is based upon regular repeating ether and imide linkage. The aromatic imide units provides stiffness, while the ether linkage allows for good melt-flow characteristic and processability. PEI exhibits inherent flame resistance and low smoke generation without the use of additives, and is used in automotive and electronics parts, composites, and wire and cable insulation (Zimmerman and Jones, 1994).

#### **3.4.1 Tensile Fracture Surface of Polyetherimide**

The characteristic behaviors of PEI in tensile test were observed by SEM. The PEI first uniformly extended, then experienced drawing with the formation of a neck, and then fractured. A small whitened area indicating void of necking rupture was observed. The mirror area where the fracture initiated, and propagated into the transition region. The rough region was often found in the fracture surface. Figure 3.17 shows an SEM image of the mirror region and the transition region, and the rough region was shown in Figure 3.18.

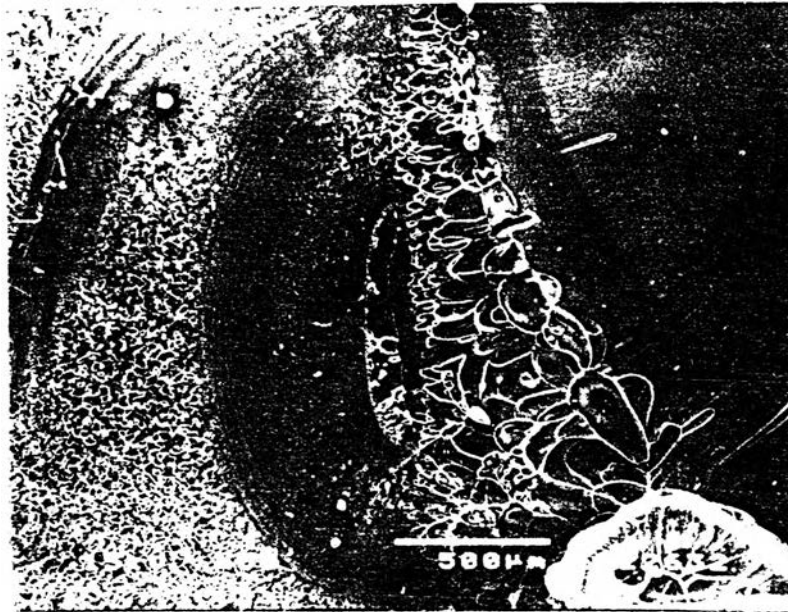


**Figure 3.17** SEM photograph showing transition region of tensile fracture surface of PEI.



**Figure 3.18** SEM photograph showing rough region of tensile fracture surface of PEI.

Crazing is a precursor of crack formation and represents a means for strain energy release. The differences in the appearance of the specimen in the rough region can be attributed to this crazing where the fibrils have become oriented or aligned as shown in Figure 3.18. Since crazing is a precursor of crack formation, it is an ideal path for crack propagation which is displayed in the fracture on this surface (Zimmerman and Jones, 1994).

There are two principal types of behavior. That may occur in the specimen, necking rupture and brittle fracture. The brittle fracture is initiated with the rib marking, as shown in Figure 3.21. The rib marking is a true crack front marking produced when a moving crack is stopped (So, 1988). After that the rough region attributed to crazes is generated. The rough region has hackles and parabolic markings. Moreover the materials in both fracture surfaces were partially void. It was found that the necking rupture showed the crack front curve and each curve generated the hackle lines with stress whitening.

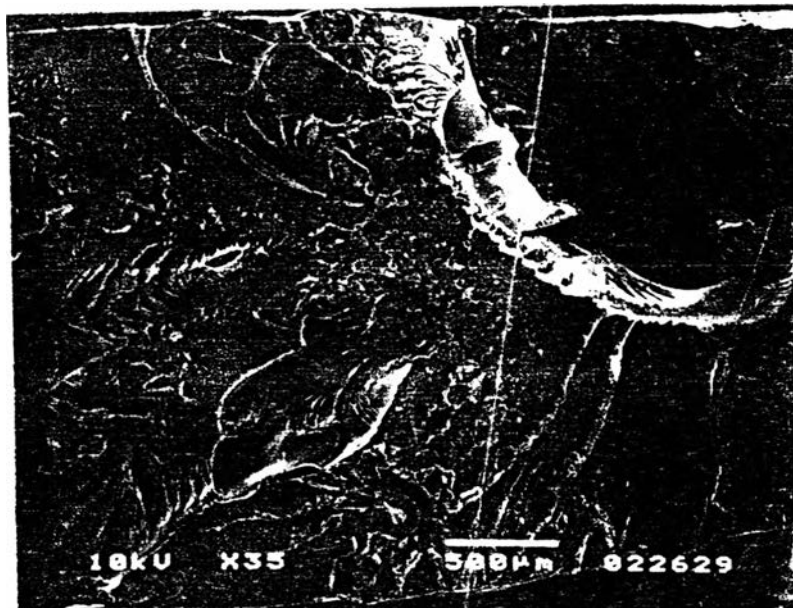


Figure 3.19 SEM photograph of tensile fracture surface of PEI.

### 3.4.2 Impact Fracture Surface of Polyetherimide

The crack morphology initiated by the mirror region and the crack propagated by crack front curve and showed so many small craze and void with stress whitening as shown in Figure 3.21(a). Figure 3.20(b) illustrate ductile deformed films and fibrils were formed on the fracture surface. Altogether, this is a low-deformation fracture with the characteristic feature of impacted fracture (Engel et al., 1981). The last region of the Izod impact specimen illustrated the smooth region due to fast fracture at the end of crack growth.

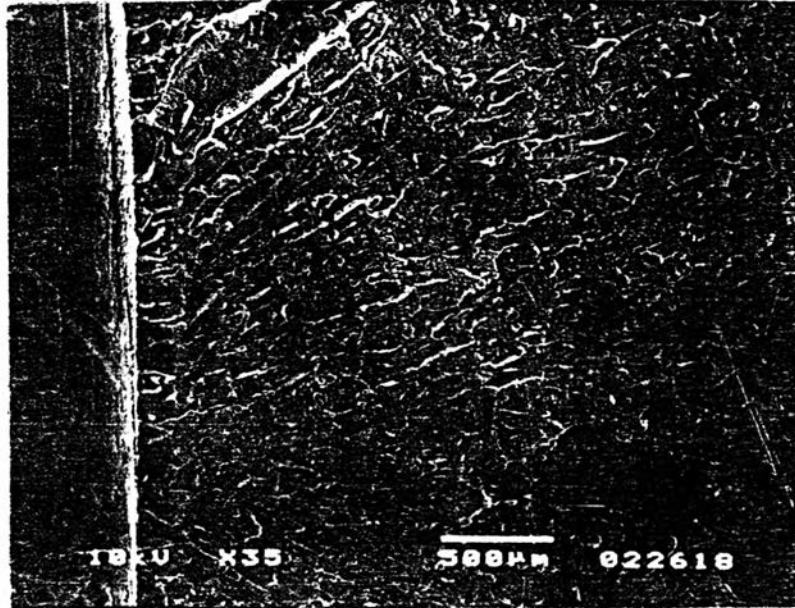
### 3.4.3 Effects of Processing History

SEM of fracture surfaces of both virgin and after reprocessed PEI showed differences in morphology. These corresponded with impact strengths, 44.8 J/m and 34.6 J/m for virgin and reprocessed materials respectively. Figures 3.22(a) and 3.23(a) show the differences between the two materials.

The mirror region appeared at the fracture origin of both materials, but was reduced after reprocessing 10 passes. The reprocessed materials showed much more stress whitening on the fracture surface. Such whitening is believed to result from refractive index changes occurring as a result of molecular chain orientation in the slowly advancing fatigue crack-tip plastics zone (Collyer, 1994 and So, 1988). The stress whitening in the impact fracture surface appeared with small hackle lines. Also some contained a smooth area with Wallner lines as seen in Figure 3.21(b). The divergent lines were more easily recognized from the middle to the end of the fracture surface. The stress whitening was also observed at the edge of outward divergent lines

along the crack direction. Furthermore, the area in each hackle contained small divergent lines as well as Wallner lines.

a



b

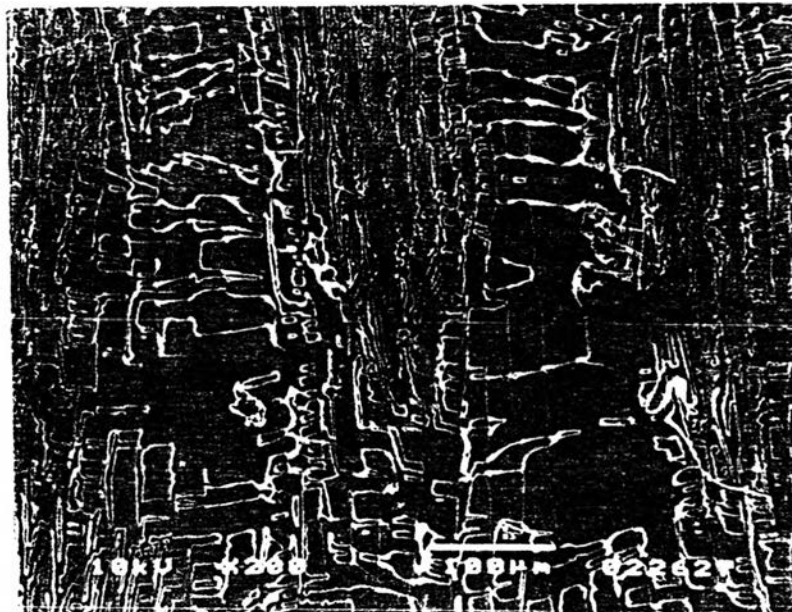
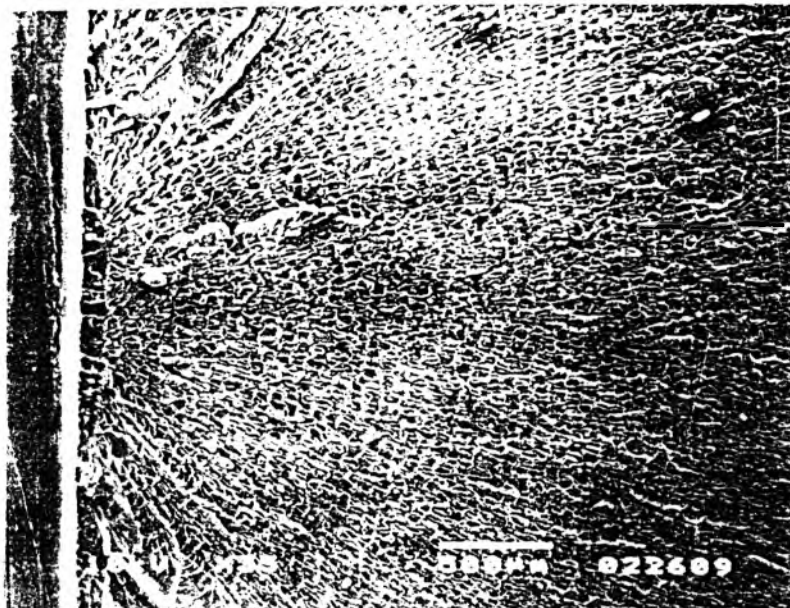


**Figure 3.20** SEM photograph of impact fracture surface of PEI (a) showing area near the notch (b) showing the latter field along the crack direction.

a



b

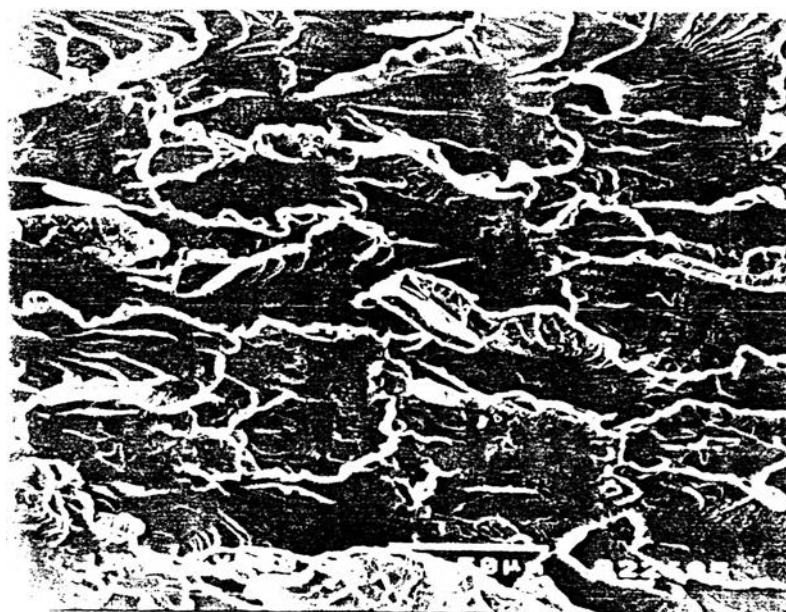


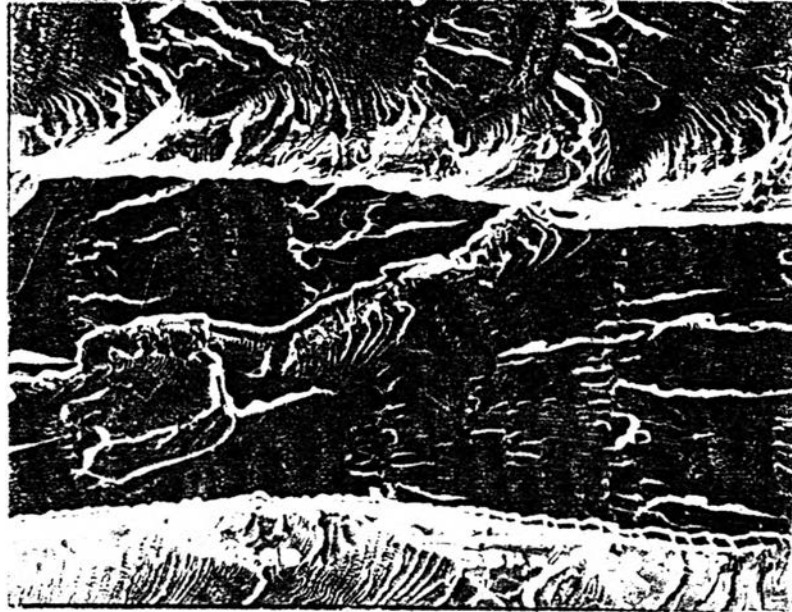
**Figure 3.21** SEM photograph of impact fracture surface of reprocessed PEI  
(a) x35 (b) x500.

Wallner lines are sometimes observed as faint striations on otherwise smooth fractures. They are formed when stress waves reflect from the specimen boundaries similar to front marking. Thus Wallner lines are not true crack fronts (So, 1988). The Wallner lines are interspersed among the hackle lines in Figure 3.22(a) and are shown at higher magnification in Figure 3.22 (b).

The Wallner lines in PEI are similar to the discontinuous growth bands of HDPE, but Wallner lines are observed in a small width of only 5  $\mu\text{m}$ . Typically, the curved markings of Wallner lines in PEI are similar to crack front markings in HDPE, with fracture initiation site located on their concave side. The discontinuous growth bands in HDPE are true crack front marking because they are produced during repetition of crack extension and arrest (So, 1988).

The large difference in crack morphology between the virgin and reprocessed PEI may be a result of the differences topological entanglement. The breakdown of the entanglement network (by chain slippage or chain rupture) plays an important role for craze formation and growth. There are two degradative mechanisms, the slipping hypothesis or disentanglement that is important at high temperatures, and chain scission occurs for higher molecular weights or crosslinked samples (Brostow and Corneliussen, 1989). So the chain disentanglement may be a major effect causing differences in the fracture surface morphology after reprocessing. Processing of the materials at high temperature allowed the chains to flow easily and also cause the chain disentanglement or chain slippage during the processed operation. This is consistent with the apparent viscosity data that showed dramatic reduction after reprocessing.

a



b

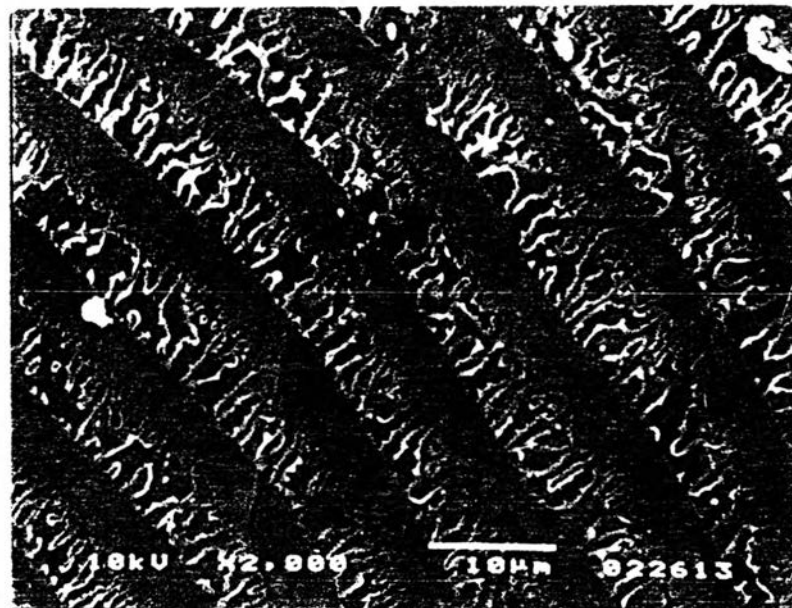


**Figure 3.22** SEM photograph of impact fracture surface of PEI showing the Wallner lines (a) interspersed in hackle lines (b) at higher magnification.